ACS OMEGA

http://pubs.acs.org/journal/acsodf

Article

Experimental Investigation of Soapstone and Granite Rocks as Energy-Storage Materials for Concentrated Solar Power Generation and Solar Drying Technology

Lilian Deusdedit Kakoko, Yusufu Abeid Chande Jande, and Thomas Kivevele*

Cite This: *ACS Omega* 2023, 8, 18554−18565

Read Online

ACCESS | Metrics & More | Article Recommendations

ABSTRACT: The intermittence of solar energy resource in concentrated solar power (CSP) generation and solar drying applications can be mitigated by employing thermal energy storage materials. Natural rocks are well recommended thermal energy storage materials as they are efficient for CSP generation. This study explores the potential of soapstone rock and also the influence of the sites' geo-tectonic setting to soapstone and granite rocks as thermal energy storage materials. Experimental characterization was done to investigate the thermo-chemical properties (thermal stability (TGA), crystalline phases (XRD), petrographic imaging and chemical composition (XRF), and high temperature test); the thermo-physical properties (density, porosity, specific and thermal capacity (DSC), thermal diffusivity, and conductivities (LFA)); and the thermo-mechanical properties (Young's modulus) of the rocks. Consequently, the rock with the most desired properties for thermal energy storage was the soapstone rock from the Craton geo-tectonic setting and it had a Young's modulus of 135 GPa at room temperature. At solar drying and CSP temperatures it had thermal capacities of 3.28 MJ/(m^3·K) and 4.65 MJ/(m^3·K); densities of 2.785 g/cm^3 and 2.77 g/cm^3; and conductivities of 2.56 W/(m·K) and 2.43 W/(m·K) respectively, and had weight loss of 0.75% at 900 °C. At high temperatures, only granite from Craton had visible cracks while the other 3 rocks did not show visible signs of fracture. Conclusively, soapstone and granite from Craton in the Dodoma region and Usagaran in the Iringa geo-tectonic settings exhibit significant differences in most thermo-properties.

INTRODUCTION

The employment of renewable energy systems as an alternative to energy sources that emit greenhouse gases faces a challenge of intermittency.[1] Among the renewables with that challenge is solar energy.[2] Electricity can be generated by concentrated solar power (CSP) systems by collecting solar thermal energy at high temperature.[3] This is also highly motivated by the perceived gradual depletion of fossil fuel reserves, their high cost, and environmental impacts resulting from their application.[4] Moreover, solar energy can be used to dry food crops as a means to reduce the postharvest losses and ensure food security of perishable products throughout the year.[4]

Thermal energy storage (TES) can be used to combat the intermittency, to extend the energy delivery period, and to match the energy demand and generation.[4] TES for CSP with an air−rock bed has low investment cost, high reliability and efficiency, is environmentally friendly, and does not require the use of heat exchangers.[5] The rock bed stores the solar thermal energy captured by concentrating collectors to temperatures of up to 500−600 °C as sensible heat, warming the air (working as the heat transfer fluid) to high temperatures.[5,6] The hot air boils a liquid into steam which in turn operates the generator turbines to produce electricity.[6] For applications in drying of agricultural food products TES is used at a moderate and steady temperature of around 40−75 °C.[7] For efficiency and economic values natural rocks used in thermal energy storage should have a high energy density for a higher ability to retain heat, which is a function of specific heat capacity and density, and excellent thermal conductivity for better energy transfer ability.[7] High heat capacity and density are desirable to reduce the required storage volume and containment structure costs. Thermal conductivity should be high enough to allow heat to be transferred with a small temperature gradient from the rock's exterior surface to its core. The rocks must have sufficient compressive strength to prevent the bottom-most layers from crushing under the weight of the rock above them.[7]

Rocks have been suggested as promising thermal energy storage materials.[5,8] Using rocks as a storage medium offers the potential of affordability due to the abundance and low cost of

Received: January 18, 2023
Accepted: May 4, 2023
Published: May 17, 2023

rocks. Some of the rocks that show high-energy storage potential include basalt, micro-gabbro/dolerite and granite.[9,10]

Globally, granites are the most abundant rocks in the continental crust, they are most widespread and come in a variety of properties including chemical composition and grain sizes,[10,11] and hence are expected to be most widespread across a diverse range of geo-tectonic settings. A variety of studies have shown a considerable difference in the properties of granite. In one study, Shang et al.[12] studied fine to medium grained granite rocks from China. Experimentation showed that the granite samples had only nonhydrothermal minerals such as feldspar, quartz, pyroxene, and illite, while Grirate et al.[13] studied granite samples from Morocco that were found to have hydrothermal mica similar to the granite rocks studied by Liet al.[1] Haldar and Tišljar[11] highlight the variations in granite texture from fine grained to medium grained to coarse and shows granite rocks with a variety of mineralogical composition. In the study performed by Alzahrani et al.,[14] it was noted that there was a variety in the mineral composition of the studied eight granite samples where only two had the hydrothermal mica (biotite, muscovite, and annite), five samples had the alteration minerals (zeolite, prehnite, kaolinite), and three of the eight samples had neither of the two thermally unstable groups of minerals. Granite has also been recommended as an energy storage material, for example, Singh et al.[15] suggested that granite rocks are potential material for thermal energy storage in systems of up to 800 °C.

Soapstone/steatite rocks have a very high thermal shock resistance than the majority of natural rocks[16] but has not been studied for use as a thermal energy storage material. A review study on the traditional soapstone as a cookware and culinary material by Kora[17] shows that soapstone rocks have excellent thermal properties including high specific heat capacity, high density, and high thermal resistance and are resistant to acid and alkali. It also explains that, due to these properties, soapstone has been used since ancient times for internal linings of stoves and fire chambers making cooking pots, metal casting molds, high temperature electrical components, and cladding for various types of stoves.[17] Huhta et al.[18] studied the composition and structure of magnesite soapstone in fire chambers construction, and it was observed that the durability of the rock increased with further exposure in fire. Due to these aforementioned excellent thermal properties it is relevant to investigate soapstone rocks' potential as TES materials.

Additionally, even rocks of a particular type may exhibit different properties depending on their mineralogical variations, thus potentially affecting their suitability for energy storage application.[3,9] Nahhas et al.[19] conducted experimental characterization on basalt rocks from France and Egypt. The two rocks showed a variation in the thermal energy storage potential, whereby the basalt from France had desirable properties as opposed to the basalt from Egypt. Moreover, the study on primitive basalt rocks from Spain and France could perform well as thermal energy storage materials as opposed to the evolved basalts from Egypt and Greece.[20] The thermal cycling tests and thermo-physical and mechanical experiments conducted on rhyolite rock concluded that the thermal energy storage parameters vary in a rock of a similar type.[5]

Rock variability is caused by factors such as disjointedness conditions, characteristics of the formative materials, eon and weathering and climatic conditions,[21] these factors are also dependent on geological tectonic settings. Tanzania geo-tectonic settings include the Archean Tanzanian Craton and the Proterozoic mobile zones.[22] Cratons are the most stable cores of the continental crust formed in the 2.5−4.0 Ga mostly during the Archaean eon.[23] The Tanzanian Craton comprises the Kavirondian, Nyanzian, and Dodoma supergroups, the latter supergroup being the craton basement containing the oldest rocks.[24] The Dodoma supergroup comprises granitoids including granite rocks accompanied by high and low grade metamorphic rocks including soapstone.[25] The Proterozoic geo-tectonic setting is a mobile belt as opposed to the stationery craton belt.[22] It is divided into three types; the Palaeoproterozoic mobile belts comprising Usagaran and Ubendian; Mesoproterozoic mobile belt of Karagwe-Ankolean, and the Neoproterozoic mobile belts of Mozambique and the Malagarasi supergroup.[26] Being a Palaeoproterozoic, the Usagaran is the oldest belt of all the types of the Tanzanian Proterozoic geotectonic belts[27] and is found on the South-eastern margin of the Craton[28] as shown in Figure 1. The rocks in the Usagaran mobile belt have a combination of mafic, pelitic sedimentary, and marine carbonates.[29]

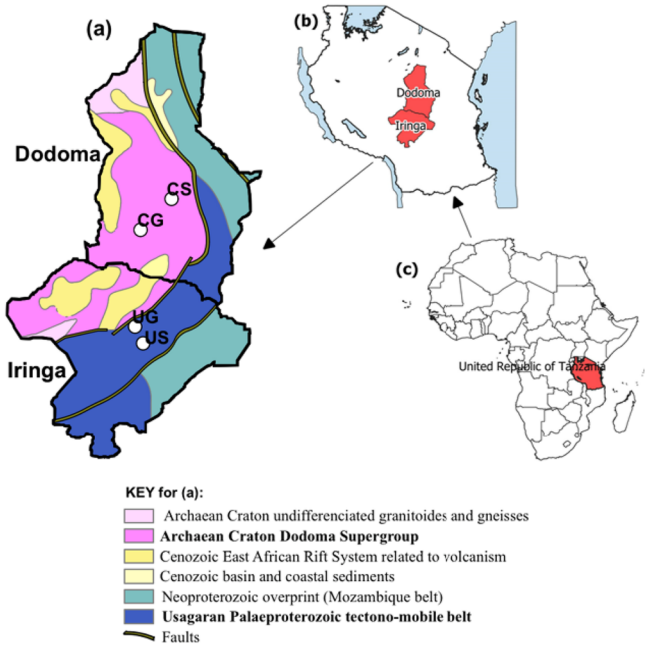

Figure 1. Map showing the location of the collected rock samples: (a) Map of Dodoma and Iringa regions showing sample collection locations and their geo-tectonic settings. (b) Map of Tanzania showing the locations of Dodoma and Iringa regions. (c) Map of Africa showing the location of Tanzania.

Therefore, this study examined the suitability of selected rocks from Tanzania, namely soapstone and granite, as media for thermal energy storage (TES) for solar drying and CSP generation application. The effect of structural and compositional variations of specific rock types on their suitability for thermal energy storage capacity application were evaluated. Soapstone and granite rock samples were obtained from the two geological settings, the Archaean Craton geo-tectonic setting in Dodoma and the Usagaran mobile belt in Iringa as shown in Figure 1. These were studied for their suitability in thermal energy storage for concentrated solar power and drying technology by investigating the thermo-physical, mechanical, and chemical properties of the rocks as sensible heat storage materials.

https://doi.org/10.1021/acsomega.3c00314
ACS Omega 2023, 8, 18554−18565

EXPERIMENTAL SECTION

Materials. The rock samples were obtained in Tanzania from two geo-tectonic settings of Craton and Usagaran as shown in Table 1. Rocks from Craton geotectonic setting were obtained from Dodoma and those from Usagaran were collected from Iringa region as shown in Figure 1. The soapstone from Craton and Usagaran were coded CS and US, respectively, and the granite from Craton and Usagaran are coded CG and UG, respectively, as shown in Table 1.

Table 1. Sample Code Names According to Geo-tectonic Setting and Rock Type

rock type	geo-tectonic setting	sample code
soapstone	Craton	CS
	Usagaran	US
granite	Craton	CG
	Usagaran	UG

The rock samples were dried in the oven at 100 °C for 5 h so as to remove both the absorbed and adsorbed water.[30] The characterization experiments on the thermo-physical, thermo-chemical and thermo-mechanical properties as related to thermal energy storage were done as summarized in Figure 2. The characterization was done for low temperatures (<150 °C) to examine the solar drying applications potential and higher temperatures (>300 °C) to examine the concentrated solar power generation potential of the rock materials.[5,7,31]

Characterization of Rock Samples. *Thermo-chemical Properties.* X-ray fluorescence technique was used to measure the oxides and elemental composition of the rocks for predicting the chemical reactions at higher temperatures and mechanical stability of the rocks,[32] whereby 1 g of pressed powder pellets of the rock samples were used in the Bruker AXS S4 spectrometer in the presence of P10 detector gas.

The crystalline evolution was measured so as to determine the available phases and predict the reactions in the rock at higher temperatures.[19] Bruker D8 ADVANCE X-ray diffractometer equipment was used to measure powdered samples of 150 μm. The equipment was fed with a primary Ge_{111} monochromator, a LinxEye silicon strip detector, and a current of wavelength 1.54059 Å from a Cu-tube. The samples were measured in the range 2° to 90° 2θ, at steps of 0.02° and a rate of 4 s per step.

Petrographic examination was conducted so as to characterize the rocks mineralogy, to identify the rock types. The rocks were cut into slices, mounted on a glass slide, and ground to the standard thin section thickness of 0.03 mm for the examination of optically transparent minerals. The petrographic characterization of the prepared specimens was achieved using a Carl Zeiss Primotech polarizing microscope equipped with built-in camera. The acquisition and manipulation of the micrographs were undertaken by the aid of MATSCOPE software.

The thermogravimetric analysis was performed for deducing the thermal stability and the volatility of the rocks' constituting materials with temperature increase.[14] About 3.5 ± 0.3 mg of <63 μm powdered sample was used in the Exstar 6000 TG/DTA 6300 machine. The process took place from 40 to 950 °C at the rate of 10 °C/min. Alumina (Al_2O_3) was used as a reference material.

A high temperature test was performed to observe the capacity of the rocks to resist fracture caused by increase in temperature up to higher temperatures.[33] Samples of 10 × 10 × 10 mm^3 were enclosed in a CBFL518C Cole Palmer Box furnace and exposed to 700 and 1000 °C for 6 h so that the rock samples could reach a steady temperature field.[19,30] They were left to gradually cool in the furnace until they reached room temperature.[33]

Thermo-physical Properties. The evolution of specific heat capacity from 20 to 950 °C was measured so as to compare the expected amount of heat stored in a unit mass.[7] Powder samples of 150 μm were used in a NETZSCH DSC 404 F1 Pegasus differential scanning calorimeter against sapphire as calibration standard. Heating was done at rate of 10 °C/min, under argon atmosphere. First the measurement for the baseline and the standard was done over the temperature range. Followed by measuring the sample and then computing the specific heat capacity according to the standard ratio method.[34] Thermal capacity was calculated as a product of density and specific heat capacity as shown in eq 1.

$$\text{thermal capacity at temp } T(C(T)) = (C_p(T)) \times (\rho(T)) \quad (1)$$

Additionally, a laser flash apparatus was used to determine the thermal diffusivity and thermal conductivity so as to understand the rates of thermal charging and discharging of the rock samples.[7] Samples of 10 × 10 × 1.5 mm^3 were placed on a graphite holder in the NETZSCH LFA 427 Microflash

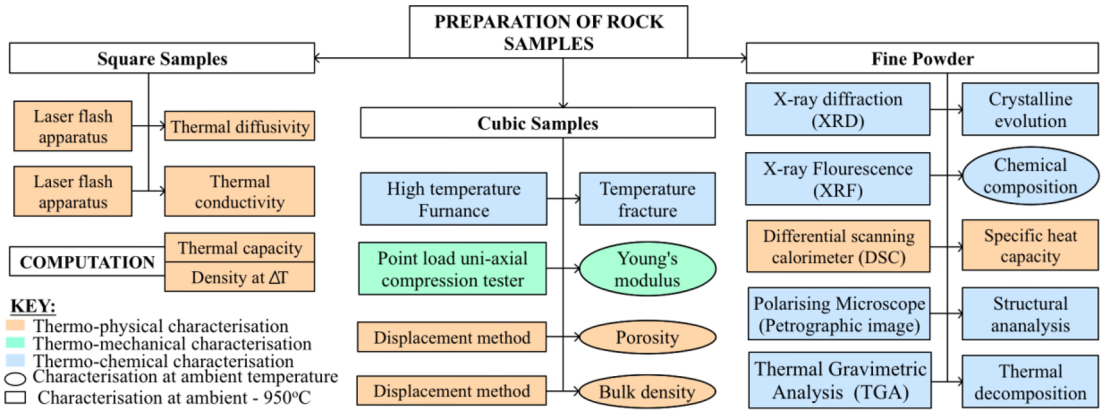

Figure 2. Characterization experiments for thermal energy storage.

https://doi.org/10.1021/acsomega.3c00314
ACS Omega 2023, 8, 18554−18565

apparatus under argon atmosphere and vacuum of 10^{-2} mBar. Heating was then done at a rate of 2.5 °C/min from ambient temperature to 950 °C.

Densities (ρ) of the four rock types were determined so as to compare the expected containment volumes of the rocks in relation to the amount of heat stored.[7] The experimentation was conducted according to the standard procedure of ASTM C128-15 by American Society for Testing and Materials ASTM[35] for Relative Density of Fine Aggregates. For each experiment, rock sample cubes of 10 × 10 × 10 mm^3 were weighed by an analytical balance to get mass W in grams. They were kept in the measuring cylinder and 50 cm^3 of water was added until the cylinder reached volume V in cm^3. The density at room temperature was then calculated using eq 2.

$$\text{density}(\rho) = \frac{W}{V - 50} \tag{2}$$

Densities at higher temperatures ($\rho(T)$) were calculated from thermal conductivity ($\lambda(T)$), thermal diffusivity ($\alpha(T)$), and specific heat capacity ($C_p(T)$) at that temperature[19] using eq 3.

$$\text{density at temp } T(\rho(T)) = \frac{(\lambda(T))}{(C_p(T)) \times (\alpha(T))} \tag{3}$$

Rock porosity was obtained so as to determine the amount of air spaces in the rock samples as they tend to affect conductance and mechanical properties of the rocks[4,36] by following the ASTM C128-15 standard procedure for absorption of fine aggregate.[35] For each experiment, rock sample cubes of 10 × 10 × 10 mm^3 were weighed by an analytical balance to get mass W in grams. They were consequently soaked in the water for 72 ± 4 h while stirring every 24 h and then surface dried and weighed to get mass M. The porosities were determined by using eq 4.

$$\text{porosity} = \frac{(M - W) \times \rho_{\text{rock}}}{W \times \rho_{\text{water}}} \tag{4}$$

Thermo-mechanical Properties. The Young's modulus was determined so as to deduce the ability of the lower layer of rocks to withstand the loading from upper layer of rocks. The nanoindentation instrumentation method was used because rocks are heterogeneous materials and its useful to get the average mechanical strength as a function of their heterogeneity.[37] Polished cylindrical samples of 5 mm diameter and 20 μm thickness were used in the nanoindentation tester NHT^3 machine with a Berkovich indenter. The experiment was done following the method by Oliver and Pharr[38] with the maximum loading of 200 Mn at a loading and unloading rate of 600 Mn/min and a Poisson's ratio of 0.3.

RESULTS AND DISCUSSION

Thermo-chemical Properties. *Chemical Composition.* Chemical composition in terms of oxide percentages was obtained using the XRF technique, and the results are shown in Figure 3. In soapstone samples, the main elements are silicon dioxide and magnesium oxide. Their dominance in the composition is caused by the dominance of talc >90%, a mineral with hydrated magnesium silicate, i.e., $Mg_3Si_4O_{10}(OH)_2$.[39,40] The most dominant elements in granite samples are silicon dioxide and aluminum oxide also resembling the findings in Srivastava et al.[32] The SiO_2 content is >65% verifying that the igneous rocks UG and CG fall in the

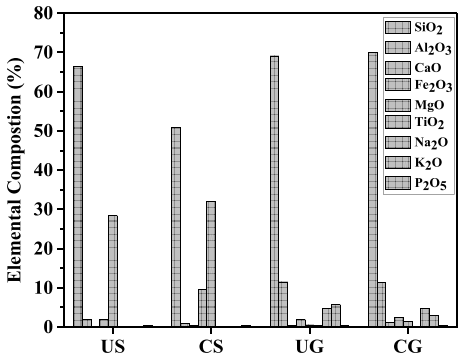

Figure 3. Oxide compositions of US, CS, UG, and CG rocks

granite rocks group; this corresponds to the observation in Maqsood et al.[41] The granite rocks are peraluminous since Al_2O_3 content is greater than the summation of Na_2O, K_2O, and CaO. This relationship corresponds to the granite compositions in Srivastava et al.[32] Sun et al.[25] also report on the presence of peraluminous granite in the Tanzania craton. Bouvry et al.[20] observed that high amounts of silicon oxides contribute to higher strength properties. Nahhas et al.[19] explain that high amounts of hematite contribute to crystallization and wide temperature range stability of the rock. The soapstone rock CS has a significant amount of Fe_2O_3 amounting to 9.65 which is higher by 7.7% as compared to US rock. Literature also report that variations in hematite levels occur in soapstone rocks and explain that most granite rocks have low Fe_2O_3.[12] Figure 3 and Table 2 show that CS has higher amounts of iron oxide, nickel, and chromium as compared to US rocks, these results were also found in Baron et al.[40] indicating that CS is an ultramafic soapstone while US is a carbonate soapstone. The carbonates in the carbonate soapstone rocks undergo chemical disintegration to form carbon dioxide at higher temperatures of 300 °C ≤ t ≤ 500 °C.[42] The carbonate nature the metamorphic rocks in Usagaran belt are due to the presence of marine carbonates deposited in the belt area.[29] Also the carbonate talc rocks are found in zones with high tectonic activities and deformation,[40] typical of the Usagaran belt as it is interrupted by tectonic faults as shown in Figure 1.

Crystalline Phases. The XRD images in Figure 4(a),(b) show the constituents of granite rock samples. The granite UG has peaks representing quartz (SiO_2), albite ($NaAlSi_3O_8$), chlorite ($(Mg, Fe, Al)_6$ $(Si, Al)_4O_{10}(OH)_8$), magnetite (Fe_3O_4), and microcline ($KAlSi_3O_8$). These minerals correspond to the microcline-rich undeformed granite rocks that are found in the Usagaran belt.[43] The rock sample CG has peaks of quartz, albite, biotite ($K(Mg, Fe)_3(AlSi_3O_{10})(F, OH)_2$), magnetite, anorthite ($CaAl_2Si_2O_8$), and muscovite/mica ($KAl_2(AlSi_3O_{10})(FOH)_2$). Muscovite and biotite are hydrothermal compounds and are thus susceptible to dehydration,[9] causing the CG rock to be unstable at elevated temperatures. Biotite was marked to be common in the magmatic rocks of the Dodoma supergroup Craton.[25]

The XRD images of soapstone rocks in Figure 4(c),(d) show that both rocks CS and US have peaks of talc, magnesite ($MgCO_3$ with iron impurities), magnesioferrite ($Mg(Fe3+)_2O_4$), magnetite and clinochlore ($(Mg,Fe^{2+})_5Al(Si_3Al)O_{10}(OH)_8$). US rock also has albite in its composition. These results correspond to the oxide compositions in Figure 4 showing the relative sources of the variability in the

https://doi.org/10.1021/acsomega.3c00314
ACS Omega 2023, 8, 18554−18565

Table 2. Elemental Composition of Soapstone Rocks

wt %	Ba	S	Mn	Cr	Zr	Co	Zn	Mo	Pb	Ni	Cu
CS	71	1021	319	719	8	307	61	2	3	1114	90
US	53	716	32	110	64	16	11	3	3	46	24

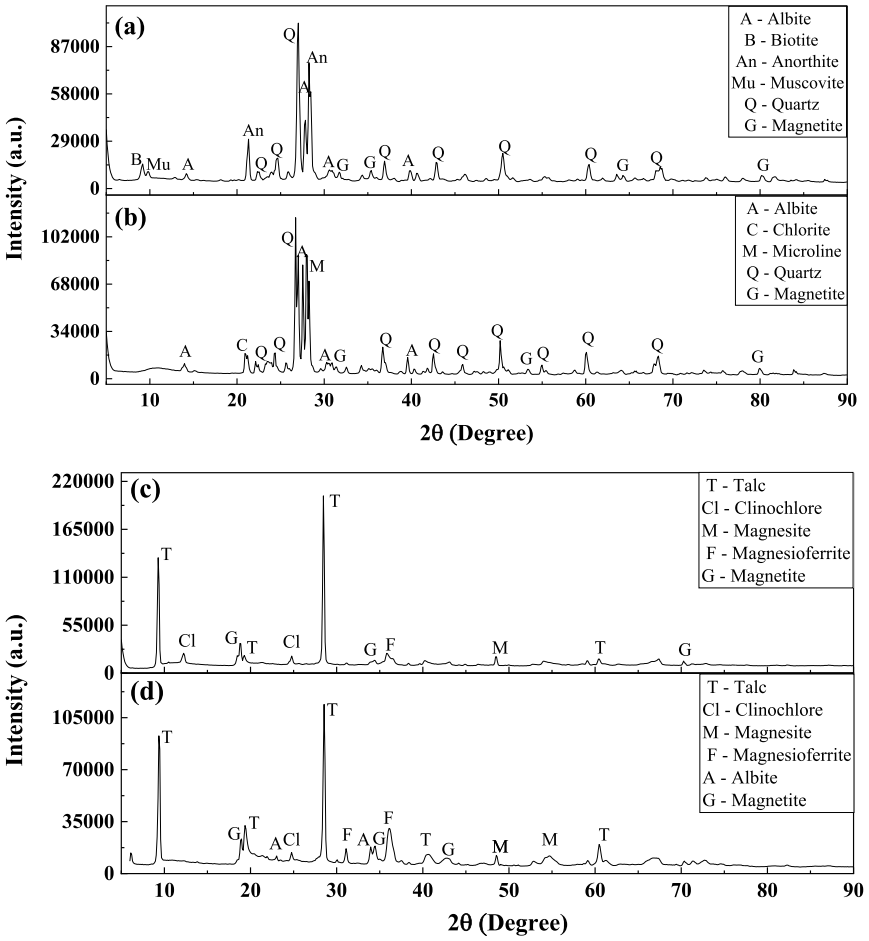

Figure 4. XRD graphs for (a) CG, (b) UG, (c) CS, and (d) US.

percentages of iron oxides in the samples. The magnesite has a potential conversion to Mg−Fe oxide and recrystallization which has a positive impact on the mechanical properties of the rock.[18] Moreover, magnesite minerals have a high density of around 5.175 g/cm^3 which contributes to high densities and thermal capacity in soapstone rocks.[9] Huhta et al.[16] also comments on the higher concentrations of magnesite and iron as a cause of elevated thermal shock resistance.

Petrographic Examination. The mineralogical compositions of the rocks are shown in Figure 5. The rock CG is a coarse to medium igneous rock composed of quartz, albite, biotite, and muscovite corresponding to a granite rock. The mineralogical composition corresponds to the findings in Figures 3, 4, and 6. The rock has black opaque areas corresponding to magnetite mineral ore. UG is a fine to medium-grained igneous rock. It is composed of albite, microcline, opaque minerals, chlorite, and quartz grains of variables sizes and shapes showing some alignment indicating that the rock is undergoing metamorphosis corresponding to the meta-granite rock. The coarse to medium grained igneous rocks can be classified as intrusive rocks and are formed by a slower cooling of magma as compared to the medium to fine grained igneous rocks reported in Nahhas et al.[19] The increase in coarseness of the grains increases the porosity of the rocks and thus negatively affects the density, thermal conductivity, and overall strength of the rocks.[41,44]

CS is a fine-grained, gray to green, soft with soapy texture, soapstone, dominantly composed of talc, with a small amount of chlorite, magnesite, magnesioferrite, and opaque (magnetite) minerals. US rock is fine-grained, gray to green, and soft with soapy texture. It has ultramylonitic foliation forming a porphyroblastic mix of inequigranular matrix of talc, magnesite, and clinochlore surrounding the recrystallized albite. The ultramylonitic deformation is usually caused by plastic deformation that may possibly be due to the rocks being located in the Kiborian shear belt of the Usagaran which created deformation events that affected the metamorphic conditions.[27] The foliation has a significant impact in reducing the thermal shock resistance of a rock[16] and leads to fracturing after several thermal cycles.[10]

Thermal Gravimetric Analysis. The weight changes with temperature for the rock samples are shown in the TGA graphs in Figure 6. The TGA for the soapstone rocks CS and US show that the soapstone rock CS shows an increase in weight until it starts to have a lower weight below its initial weight % at 900 to 950 °C (which is above the solar drying and CSP

https://doi.org/10.1021/acsomega.3c00314
ACS Omega 2023, 8, 18554−18565

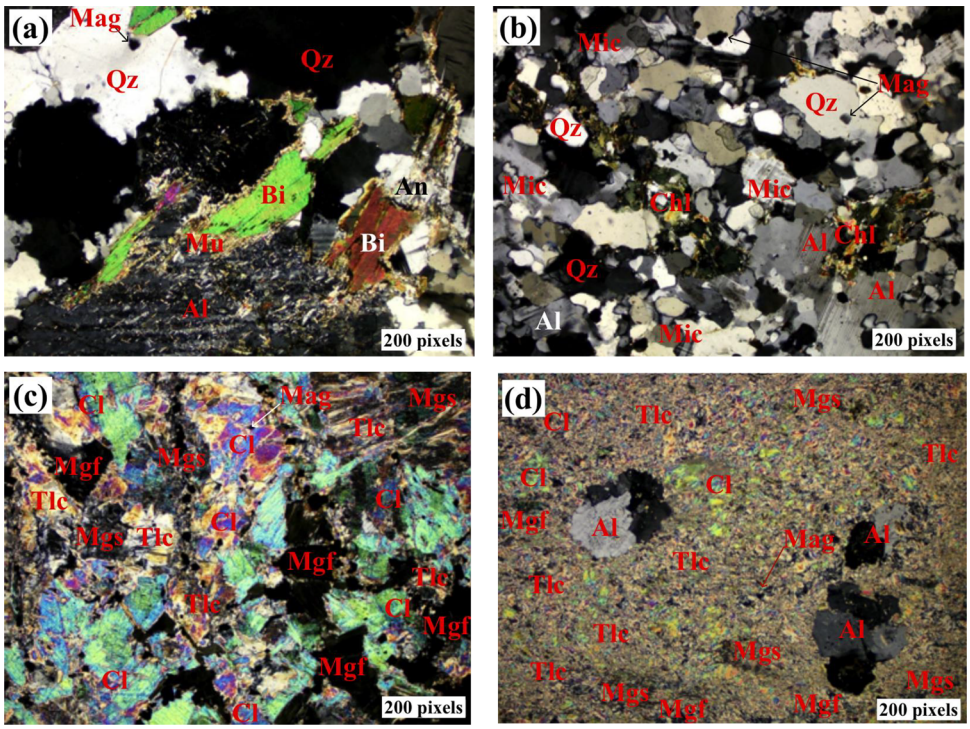

Figure 5. Petrographic image for (a) CG, (b) UG, (c) CS, and (d) US, respectively. Qz = quartz, Mu = muscovite, Bi = biotite, Al = albite, Chl = chlorite, An = anorthite, Tlc = talc, Mgs = magnesite, Cl = clinochlore, Mag = magnetite, Mgf = magnesioferrite.

temperature ranges) and it undergoes a maximum weight loss of 0.75%. The high stability of CS rock may be due to its high-grade nature (formed in high temperature and pressure conditions) and the polymetamorphism of metamorphic rocks found in the Dodoma supergroup.[45] The soapstone US is stable at solar drying temperatures but loses weight until a total of 0.4% from the original weight at the high temperatures of 350 to 600 °C with no further weight loss thereafter. This weight loss is because US is a carbonate soapstone caused by the marine carbonate sediments of the Usagaran belt.[29] The carbonate undergoes chemical disintegration at higher temperatures of 300 °C $\leq t \leq$ 500 °C to form an oxide and carbon dioxide (CO_2) that is released from the sample.[42]

The TGA for the granite CG shows that there is a steep weight decrease of 1.2% at 100−250 °C, due to the presence of muscovite and biotite, the hydrothermal compounds that dehydrate by losing chemically bound water at the boiling point.[9,14] At 900−950 °C a total of 2.6% of initial weight is lost. Granite rock UG shows no weight loss throughout the temperature increase; hence it is stable at both solar drying and CSP temperatures. It however shows an increase in weight due to the oxidation of mineral ores that are present in the sample. The trend of weight gain in granite has also been reported in ref 14.

CS, US, CG, and UG rocks show a maximum mass gain of 0.98%, 0.3%, 0.5%, and 0.3%, respectively. This is due to the oxidation reaction of magnetite mineral ore as shown in Figures 6 and 7. The magnetite reacts with oxygen from the synthetic air to form hematite both at lower temperatures and at higher temperatures.[46]

High-Temperature Test. The rock samples were heated up to a temperature of 700 and 1000 °C as shown in Figure 7. Soapstone samples had no visible cracks at both temperatures. However, granite rock CG had fractured and disintegrated at the temperature of 1000 °C, while rock UG had no visible cracks at that temperature. This may be attributed to the dehydration of the muscovite and biotite hydrothermal minerals,[9] and the varying thermal expansion between quartz and other composing minerals are a contributing factor to the cracking of the CG rock.[47] Li et al.[1] also observed that granite rock develops cracks during the first thermo-cycle.

Thermo-Physical Properties. *Density and Porosity.* Figure 8 shows that densities and porosities have an opposite relationship, where the density is lower with an increase in porosity. The densities and porosity are affected by mineral composition, chemical composition of minerals and the grain size.[41,48] The densities of CG and UG were 2.228 g/cm^3 and 2.426 g/cm^3 while the porosities were 0.97%Vol and 0.6%Vol, respectively. This is because UG has fine grains and hence a higher density and lower porosity as compared to CG rock. These porosity values of granite are in range of those mentioned in the literature, i.e., 0.8−2.6%Vol,[5,41] while the density values are slightly lower than those mentioned in the literature as shown in Table 3.

Soapstone samples have higher densities as compared to granite samples. This was also observed in Huhta[48] who explained that due to an ultramafic nature soapstone rocks tend to have elevated densities than other rocks. Also these higher densities are brought about by the presence of magnesite compound that has a density of about 5.175 g/cm^3.[9] Similarly, the densities and porosities are oppositely related. CS rock has the highest density of 2.796 g/cm^3 and the lowest porosity of 0.18%Vol, the high density and low porosity contributes to high thermal capacity of the rocks and higher thermal conductance of the rock.[4] The US rock has the highest porosity of 1.9%Vol while its density is 2.635 g/cm^3. High porosity has a negative effect on the compressive strength of rocks.[36]

The values correspond to the values reported in Hänchen et al.[49] and Tiskatine et al.[5] with the density of CS being slightly

https://doi.org/10.1021/acsomega.3c00314
ACS Omega 2023, 8, 18554−18565

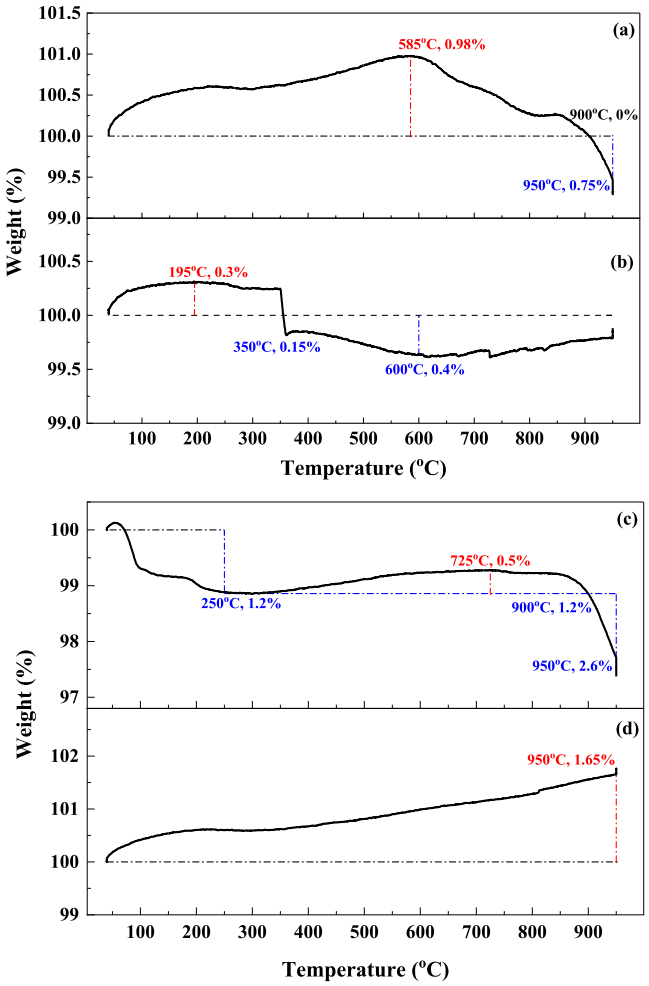

Figure 6. TGA graph for (a) CS, (b) US, (c) CG, and (d) UG.

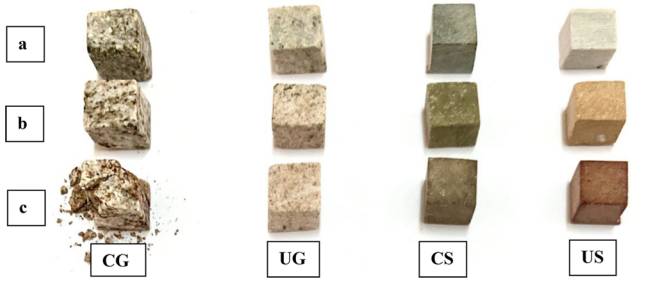

Figure 7. Rock samples: (a) ore, (b) heated at 700 °C, (C) heated at 1000 °C.

higher. As compared to that of most other rocks in Tiskatine et al.[5] the density values are in the range to most other rocks with the exception of gabbro rock that has densities of 2.9−3 g/cm^3. The highest porosity values were 8.06 %Vol for basalt rocks and 12.79 %Vol for schist rock. The quartzitic sandstone and rhyolite had the lowest porosity of 0.39 and 0.41%Vol, respectively. Table 3 shows the densities of other common TES materials, whereby the densities of cofalit and castable ceramics are slightly higher. High tension concrete has similar value with the CS rock, and the molten salts are in range with US, UG, and CG rocks.[19]

The evolution of density at low and high temperatures is as shown in Figures 9 and 10. The density increase as the

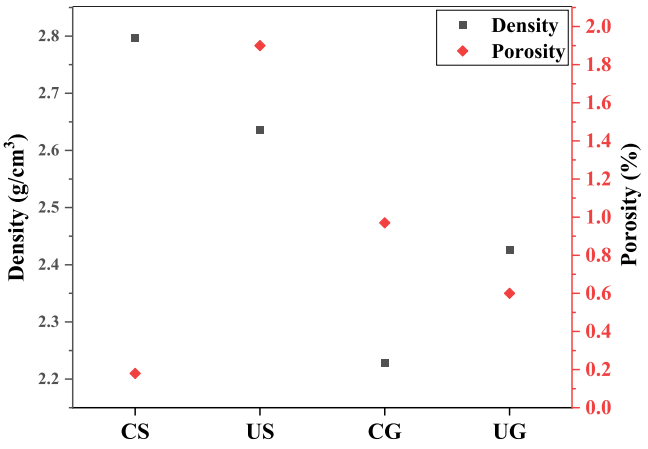

Figure 8. Density and porosity at room temperature.

temperature increases is very insignificant concurring with findings reported in ref 9. In this study the density decreases with temperature increase at a very low rate of 7.53 × 10^{-4} g/(cm^3·K) for rock CS, US, and UG and 5.91 × 10^{-4} g/(cm^3·K) for CG rock. Figure 9 shows that, at solar drying temperatures of 40−75 °C, the measured densities were 2.785 g/cm^3, 2.635 g/cm^3, 2.225 g/cm^3, and 2.420 g/cm^3 for CS, US, CG, and UG, respectively, showing a slight decrease from the density at room temperature. The densities at CSP temperatures of 500−600 °C for rocks CS, US, CG, and UG were 2.77 g/cm^3, 2.60 g/cm^3, 2.2 g/cm^3, and 2.4 g/cm^3, respectively, as shown in Figure 10. Zhu et al.[50] observed the decrease of density with temperature as a courtesy of rock mass loss and volume increase due to expansion. In granite for example, the increase in volume is the leading factor due to high expansion rates of the composing minerals especially quartz.[47,50]

Specific Heat Capacity and Thermal Capacity. Specific heat capacities of the four samples are shown in Figure 11 from which it can be observed that soapstone and granite rocks exhibit almost the same values. These similarities have also been reported in ref 51, where magmatic and metamorphic rocks exhibited almost the same values of specific heat capacity with temperature changes. The magmatic granite rock samples CG and UG had the same values and trends to both metamorphic soapstone rock samples CS and US. Their evolution with temperature is as shown in Figure 14, where the specific heat capacities increase with temperature. The increase in specific heat capacity at higher temperatures is slight, Nahhas et al.[19] states that the slight increase is due to the Dulong-Petit law defining that the increase will eventually reach a constant value at higher temperatures. At 20 °C the specific heat capacity of soapstone rock is 1.074 J/g·K and of the granite rock is 1.07 J/g·K. The increase in values between 200 and 300 °C is unexpectedly low, this was also observed by El Alami et al.,[9] and it was due to silanol transformation in which silicon hydroxide is converted to silicon oxide and aqua; the latter then evaporates.

As compared to most other rocks shown in Table 3 the specific heat capacity values of the experimented rocks at room temperature are higher. The values are approximately in range with those of granodiorite, gabbro, basalt, and schist. The specific heat capacities of other common TES materials such as high-tension concrete and castable ceramics are slightly lower, cofalit has approximately similar values as the experimented

https://doi.org/10.1021/acsomega.3c00314
ACS Omega 2023, 8, 18554−18565

Table 3. Thermo-physical Properties of Various TES Materials at 20 °C from Literature

	density (g/cm^3)	specific heat (J/g·K)	thermal capacity MJ/(m^3·K)	thermal conductivity (W/m· K)	ref
molten salts	0.9−2.6	1.5	1.35−3.9	0.15−2	19
cofalit	3.12	0.8−1.03	2.5−3.22	1.4−2.1	
castable ceramics	3.5	0.866	3.03	1.35	
HT concrete	2.75	0.916	2.52	1	
		ROCKS			
granite	2.6−2.7	0.6−0.95	1.56−2.52	2.6−3.1	5
limestone	2.3−2.8	0.68−0.91	1.58−2.51	2.0−3.0	
marble	2.6−2.7	0.8−0.88	2.08−2.37	2.3−3.2	
quartzite	2.5−2.6	0.62−0.83	1.56−2.19	2.9−5.7	
sandstone	2.2−2.6	0.69−0.95	1.49−2.51	1.7−2.9	
granodiorite	2.7	0.65−1.020	1.74−2.78	2.1−2.6	
gabbro	2.9−3.0	0.6−1	1.72−3.03	1.5−2.6	
basalt	2.3−3.0	0.7−1.23	1.60−3.71	1.2−2.3	
hornfels	2.7	0.82	2.25	1.5−3.0	
schist	2.6−2.8	0.790−1.1	2.09−3.08	2.1−3.0	
quartzitic sandstone	2.6−2.6	0.652	1.71−1.72	5.0−5.2	
rhyolite	2.3−2.6	0.785	1.81−2.04	1.6−2.3	
andesite	2.6−2.7	0.815	2.13−2.17	2.3−2.8	
calcareous sandstone	2.7	0.652	1.73	4.4	
steatite/soapstone	2.7−3.0	0.98−1.07	2.63−3.18	2.5	
dolerite	2.7−2.9	0.87−0.9	2.31−2.61	2.2−3.0	
gneiss	2.7	0.77−0.98	2.08−2.64	2.7−3.1	
diorite	2.8−3.0	1	2.8−3	2.5	
dolomite	2.8	0.80	2.21−2.27	2.1	

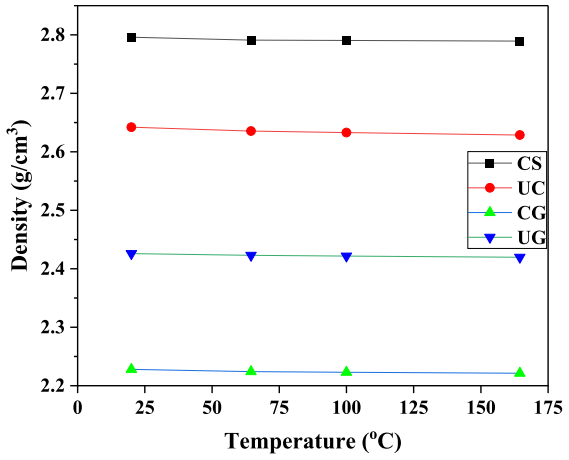

Figure 9. Evolution of density at low temperatures.

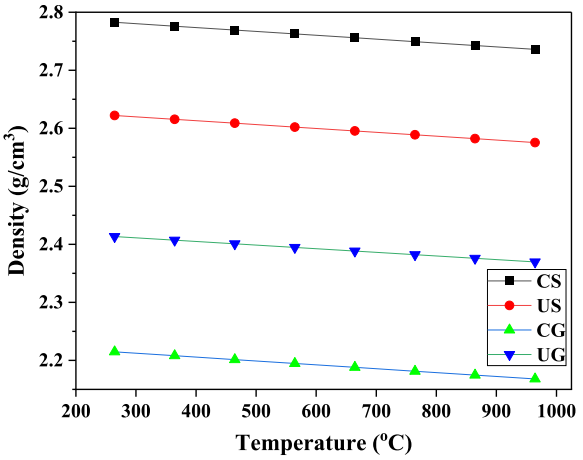

Figure 10. Evolution of density at high temperatures.

rocks, while the molten salts have higher values than the experimented rocks.

Thermal capacity evolution with temperature are as shown in Figures 12 and 13, since the thermal capacity is volumetric and the density changes very slightly with temperature the thermal capacity evolution follows almost the same profile as the specific heat capacity. However, the higher is the density the higher is the thermal capacity; hence, the soapstone rocks exhibited higher values as compared to the granite rocks. The thermal capacities of rocks CS, US, CG, and UG were 3.0 MJ/(m^3·K), 2.83 MJ/(m^3·K), 2.4 MJ/(m^3·K) and 2.6 MJ/(m^3·K), respectively, at 20 °C. All other common TES materials have ranging or slightly higher thermal capacity values as shown in Table 3. The table also shows that quartzitic and calcareous sandstone, rhyolite, andesite, and hornfels rocks have lower values than CS, US, CG, and UG rocks, while other rocks have almost similar values as gabbro, basalt, and schist with a potential of having slightly higher values than CS.

At solar drying temperatures the thermal capacities ranged at 3.12−3.28 MJ/(m^3·K), 2.94−3.1 MJ/(m^3·K), 2.48−2.62 MJ/(m^3·K) and 2.7−2.84 MJ/(m^3·K) for CS, US, CG, and UG, respectively, as shown in Figure 12. As the thermal capacities increase with temperature the values for concentrated power generation application are also higher as shown in Figure 13. These values ranged at 4.45−4.65 MJ/(m^3·K), 4.25−4.45 MJ/(m^3·K), 3.55−3.8 MJ/(m^3·K), and 3.9−4.15 MJ/(m^3·K) for CS, US, CG, and UG, respectively.

Thermal Diffusivity and Conductivity. Thermal diffusivity of the samples decreases with temperature as shown in Figures 14 and 15. This observation has also been reported in ref 9. The diffusivity values of soapstone are higher than those of granite at room temperature and at elevated temperatures. Lower values of diffusivity imply that the rock has a tendency

https://doi.org/10.1021/acsomega.3c00314
ACS Omega 2023, 8, 18554−18565

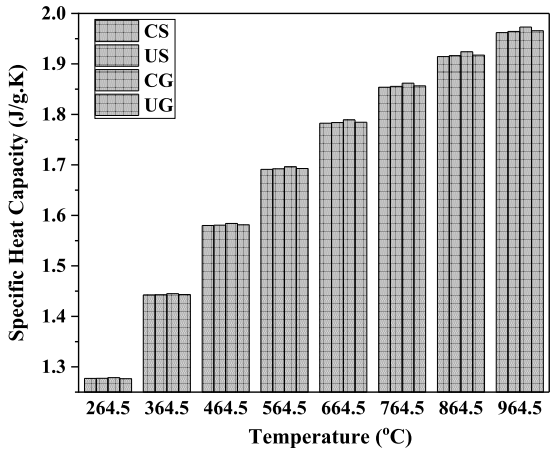

Figure 11. Evolution of specific heat capacity with temperature.

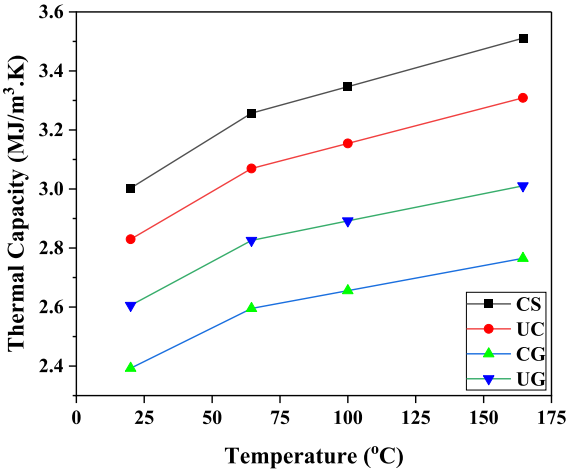

Figure 12. Evolution of thermal capacity at low temperatures.

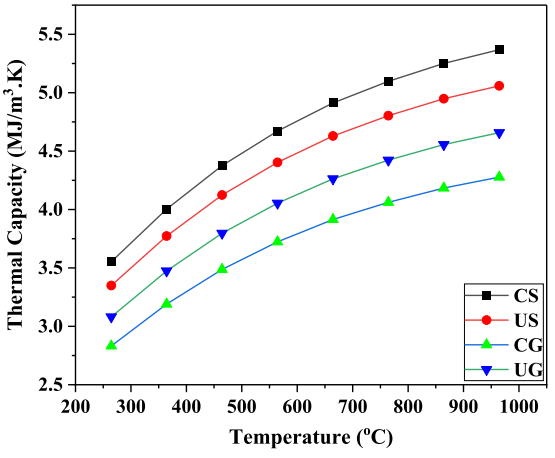

Figure 13. Evolution of thermal capacity at higher temperatures.

to absorb heat as opposed to transmitting it for the required use.[19] At 20 °C soapstone diffusivity values for CS and US samples are 0.86 mm^2/s and 0.77 mm^2/s, respectively, while the values for granite samples CG and UG at the same temperatures are 0.70 mm^2/s and 0.73 mm^2/s. At 300 °C the diffusivity of CS, US, CG, and UG falls at a difference of 0.2 mm^2/s, 0.18 mm^2/s, 0.14 mm^2/s, and 0.18 mm^2/s, respectively. Making the average rate of change of diffusivity

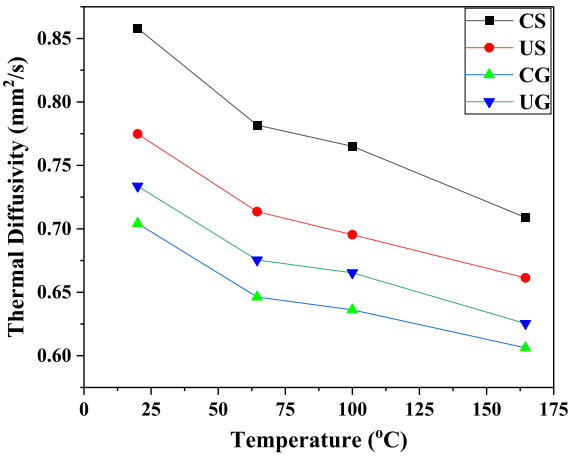

Figure 14. Thermal diffusivity at low temperatures.

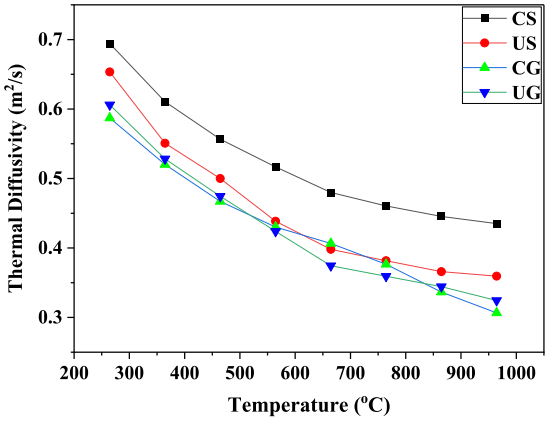

Figure 15. Thermal diffusivity at high temperatures.

to be 0.001 $mm^2/s{\cdot}°C$ for soapstone and 0.0008 $mm^2/s{\cdot}°C$ for granite. This is because the rate of decrease is higher for rocks with higher values at room temperature as opposed for those with lower values.[9]

Figure 14 shows that at 40−75 °C where solar drying is convenient, the diffusivity of the rocks decreases up to a range of 0.825−0.775 mm^2/s, 0.745−0.71 mm^2/s, 0.675−0.645 mm^2/s and 0.705−0.67 mm^2/s for of CS, US, CG, and UG, respectively. Figure 15 displays that although the rate of decrease in diffusivity of soapstone is higher than of granite, the overall diffusivity values for granite at 300 °C are relatively lower than those of soapstone. At CSP temperatures ranging 500−600 °C, the diffusivity of the rocks ranges at 0.54−0.505 mm^2/s, 0.48−0.425 mm^2/s, 0.45−0.4.5 mm^2/s, and 0.455−0.42 mm^2/s for CS, US, CG, and UG, respectively. At 700 °C and above the diffusivity of soapstone CS is highest while the diffusivity of soapstone US is almost similar to that of granite UG and CG. The high diffusivity at higher temperatures in CS may be attributed to the presence of hematite in soapstone CS.[19]

Thermal conductivity for the four samples is as shown in Figures 16 and 17. The thermal conductivity generally decreased with temperature. This is caused by the crystalline nature of the rocks as shown in the peaks of the XRD in Figure 4. Nahhas et al.[19] explain that for crystalline rocks the conductivity decreases with temperature as opposed to the amorphous rocks in which the diffusivity usually increases with temperature. Thermal conductivities at 20 °C were 2.58 W/

https://doi.org/10.1021/acsomega.3c00314
ACS Omega 2023, 8, 18554−18565

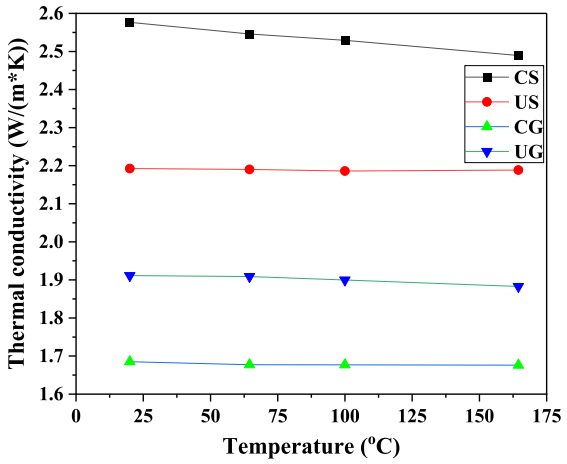

Figure 16. Thermal conductivity at low temperatures.

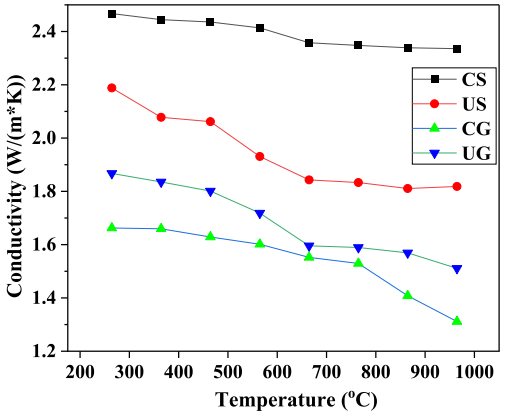

Figure 17. Thermal conductivity at high temperatures.

(m·K) and 2.19 W/(m·K) for soapstone CS and US, respectively, while those of granite CG and UG were 1.69 W/(m·K) and 1.91 W/(m·K). The conductivities for soapstone were higher than those of granite. Most other rocks shown in Table 3 have thermal conductivities approximately similar or slightly higher to that of the experimented rocks with the exceptions of quartzitic and calcareous sandstones that have higher values. Other common TES materials shown in Table 3 have lower conductivity values than all the four experimental values

As displayed in Figure 16, at lower temperatures the rate of decrease of thermal conductivity is higher in CS rocks than in the other three rocks but, at higher temperatures shown in Figure 17, its rate of decrease is the lowest compared to US, CG, and UG rocks. Chen et al.[30] explained that the rate of decrease of thermal conductivities is dependent on the its values at room temperature, whereby conductivities between 2.5 and 3.5 W/(m·K) will show a linear decrease while those below 2.5 W/(m·K) will have a minor decrease at lower temperature and a significant decrease at higher temperatures. Thus, the soapstone sample CS showed significantly higher conductivity values at higher temperatures as compared to US, CG, and UG rocks. At 40−75 °C (solar drying temperatures) the average conductivities of CS, US, CG, and UG are 2.56 W/(m·K), 2.19 W/(m·K), 1.65 W/(m·K) and 1.95 W/(m·K) respectively, see Figure 16. At CSP temperatures of 500−600 °C the conductivity values for the rocks as shown in Figure 17 were 2.42 W/(m·K), 2 W/(m·K), 1.6 W/(m·K), and 1.72 W/(m·K), respectively, confirming that the rate of heat transfer in rocks is expected to be higher during solar drying applications than in CSP applications.

Thermo-mechanical Properties. *Young's Modulus.* Figure 18 shows the Young's modulus of the four rock

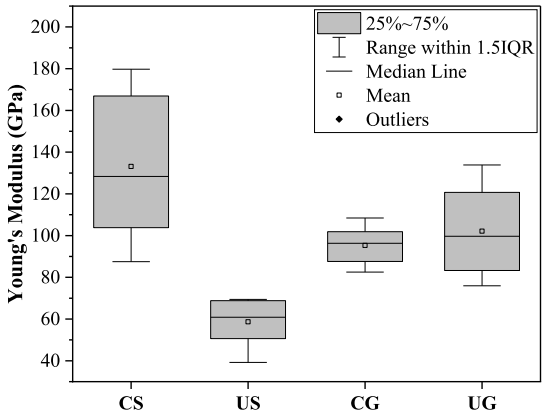

Figure 18. Young's modulus at room temperature.

samples as a measure of their mechanical strength on point loading since point loads are usually higher than overall distributed loading in rock beds.[10] Despite its high heterogeneity, the soapstone rock CS had the highest value of 135 GPa followed by the granite rocks UG and CG that have Young's modulus mean values of 95 and 104 GPa, respectively. The values of Young's modulus for CS, CG, and UG are above 80 GPa, a value that was recommended by Nahhas et al.[19] for TES materials. However, the soapstone rock US has a low unrecommended value of 60 GPa, and this is due to its meta-sedimentary nature of its origin and its high porosity.[22,36]

CONCLUSIONS

The collected data show a significant difference between the soapstone and granite rocks from Craton and Usagara geotectonic settings. The chemical compositions in granites had less variation as opposed to the mineral composition where CG contained hydrothermal minerals and UG had only thermally stable minerals. Soapstone had a variation in chemical compositions that confirmed that CS is an ultramafic rock and US a carbonate soapstone, however, they had similar minerals that varied only in terms of intensities. As a result, the TGA showed that maximum weight loss for CG, US, and CS were 1.2% at 100−250 °C, 0.4% at 250−350 °C, 0.75% at 950−980 °C, while UG had no weight loss throughout the temperature range of 40−950 °C. The premature chemical disintegration in CG and US was due to the loss of water in the hydrothermal minerals and the decomposition of carbonates into carbon dioxide, respectively. The Young's modulus for US, CG, UG, and CS at room temperature was at 60, 95, 104, and 135 GPa. The energy densities (thermal capacities) and the rates of heat transfer (thermal conductivities) were consistently at CS > US > UG > CG. At solar drying temperatures, the thermal capacities and conductivities ranged at 2.7−3.28 MJ/(m^3·K) and 1.91−2.56 W/(m·K), respectively. At CSP temperatures the values were 3.9−4.65 MJ/(m^3·K) and 1.68−2.43 W/(m·K). CG rock fractured and disintegrated during the high temperature fracture test at 1000 °C while CS, UG, and US showed no cracks. The overall results show

https://doi.org/10.1021/acsomega.3c00314
ACS Omega 2023, 8, 18554−18565

thermal properties for both soapstone and granite vary with geo-tectonic settings and are site specific. The soapstone from craton (CS) have good performance as a thermal energy storage material for both CSP and solar drying surpassing the other three rocks in terms of thermal capacity and conductivities which contribute to good absorption, hence good storage and transmission of heat per degree change in temperature. It also has good chemical stability at higher temperatures and has the highest mechanical strength. The soapstone from Usagara had the second-best thermal capacity and thermal conductivities, but are susceptible to deterioration at elevated temperatures and have the lowest mechanical strength and thus are easiest to disintegrate due to rock-bed loading. UG rock has low thermal capacity and conductivity thus needing a high temperature change to store an equal amount of energy to the soapstone rocks. Despite its good mechanical and chemical properties, it is insufficient for solar drying since high temperatures above 75 °C negatively impact the nutritional values of the dried foods. In addition to these drawbacks, the CG rock undergoes chemical disintegration at solar drying temperatures. There is a need to conduct further experimentation to examine the actual TES performance capacity of these rocks.

AUTHOR INFORMATION

Corresponding Author

Thomas Kivevele − *School of Materials, Energy, Water and Environmental Sciences (MEWES), Nelson Mandela African Institution of Science and Technology (NM-AIST), P.O. Box 447 Arusha, Tanzania*; Email: thomas.Kivevele@nm-aist.ac.tz

Authors

Lilian Deusdedit Kakoko − *School of Materials, Energy, Water and Environmental Sciences (MEWES), Nelson Mandela African Institution of Science and Technology (NM-AIST), P.O. Box 447 Arusha, Tanzania; School of Architecture, Construction Economics and Management (SACEM), Ardhi University (ARU), P.O. Box 35176 Dar es salaam, Tanzania;* orcid.org/0009-0003-7379-7321

Yusufu Abeid Chande Jande − *School of Materials, Energy, Water and Environmental Sciences (MEWES), Nelson Mandela African Institution of Science and Technology (NM-AIST), P.O. Box 447 Arusha, Tanzania;* orcid.org/0000-0002-0106-2081

Complete contact information is available at: https://pubs.acs.org/10.1021/acsomega.3c00314

Notes

The authors declare no competing financial interest.

ACKNOWLEDGMENTS

The authors highly acknowledge financial support from the project titled "Solar dryer integrated with energy storage system: An energy efficient and environmentally friendly technology for drying biomaterials in Tanzania" with reference no. 9-257. The project is coordinated by the Partnerships for Enhanced Engagement in Research (PEER) through funds from the United States Agency for International Development (USAID).

REFERENCES

(1) Li, B.; Ju, F.; Xiao, M.; Ning, P. Mechanical stability of granite as thermal energy storage material: An experimental investigation. *Engineering Fracture Mechanics* **2019**, *211*, 61−69.

(2) Wang, K.; Qin, Z.; Tong, W.; Ji, C. Thermal energy storage for solar energy utilization: Fundamentals and applications. *Resources, Challenges and Applications* **2020**, *415*, No. 91804, DOI: 10.5772/intechopen.91804.

(3) Adeleke, A.; Airoboman, A. A Review on Packed Bed of Rock as Thermal Energy Storage for Concentrated Solar Power Plant. *International Journal of Engineering Research* **2019**, *8*, 121−130.

(4) Kant, K.; Shukla, A.; Sharma, A.; Kumar, A.; Jain, A. Thermal energy storage based solar drying systems: A review. *Innovative food science & emerging technologies* **2016**, *34*, 86−99.

(5) Tiskatine, R.; Oaddi, R.; El Cadi, R. A.; Bazgaou, A.; Bouirden, L.; Aharoune, A.; Ihlal, A. Suitability and characteristics of rocks for sensible heat storage in CSP plants. *Sol. Energy Mater. Sol. Cells* **2017**, *169*, 245−257.

(6) Py, X.; Sadiki, N.; Olives, R.; Goetz, V.; Falcoz, Q. Thermal energy storage for CSP (Concentrating Solar Power). *EPJ. Web of Conferences* **2017**, *148*, 00014.

(7) Bal, L. M.; Satya, S.; Naik, S. N. Solar dryer with thermal energy storage systems for drying agricultural food products: A review. *Renewable & Sustainable Energy Reviews* **2010**, *14*, 2298−2314.

(8) Alva, G.; Liu, L.; Huang, X.; Fang, G. Thermal energy storage materials and systems for solar energy applications. *Renewable and Sustainable Energy Reviews* **2017**, *68*, 693−706.

(9) El Alami, K.; Asbik, M.; Agalit, H. Identification of natural rocks as storage materials in thermal energy storage (TES) system of concentrated solar power (CSP) plants − A review. *Sol. Energy Mater. Sol. Cells* **2020**, *217*, No. 110599.

(10) Allen, K.; von Backström, T.; Kröger, D. G.; Kisters, A. Rock bed storage for solar thermal power plants: Rock characteristics, suitability, and availability. *Sol. Energy Mater. Sol. Cells* **2014**, *126*, 170−183.

(11) Haldar, S. K.; Tišljar, J. Chapter 4 - Igneous Rocks. In *Introduction to Mineralogy and Petrology*; Haldar, S. K., Tišljar, J., Eds.; Elsevier, 2014; pp 93−120.

(12) Shang, X.; Zhang, Z.; Xu, X.; Liu, T.; Xing, Y. Mineral Composition, Pore Structure, and Mechanical Characteristics of Pyroxene Granite Exposed to Heat Treatments. *Minerals* **2019**, *9*, 553.

(13) Grirate, H.; Zari, N.; Elamrani, I.; Couturier, R.; Elmchaouri, A.; Belcadi, S.; Tochon, P. Characterization of several Moroccan rocks used as filler material for thermal energy storage in CSP power plants. *Energy Procedia* **2014**, *49*, 810−819.

(14) Alzahrani, A. M.; Lasheen, E. S. R.; Rashwan, M. A. Relationship of Mineralogical Composition to Thermal Expansion, Spectral Reflectance, and Physico-Mechanical Aspects of Commercial Ornamental Granitic Rocks. *Materials* **2022**, *15* (6), 2041.

(15) Singh, H.; Saini, R.; Saini, J. A review on packed bed solar energy storage systems. *Renewable and Sustainable Energy Reviews* **2010**, *14* (3), 1059−1069.

(16) Huhta, A.; Kärki, A.; Hanski, E. A new method for testing thermal shock resistance properties of soapstone-Effects of micro-structures and mineralogical variables. *Bulletin of the Geological Society of Finland* **2016**, *88* (1), 21.

(17) Kora, A. J. Traditional soapstone storage, serving, and cookware used in the Southern states of India and its culinary importance. *Bulletin of the National Research Centre* **2020**, *44* (1), 83.

(18) Huhta, A.; Tuisku, P.; Balic-Zunic, T.; Kärki, A. Magnesite soapstone in use of fire chamber constructions: composition and structure adaptation. *Bulletin of the Geological Society of Finland* **2019**, *91*, 101.

(19) Nahhas, T.; Py, X.; Sadiki, N. Experimental investigation of basalt rocks as storage material for high-temperature concentrated solar power plants. *Renewable and Sustainable Energy Reviews* **2019**, *110*, 226−235.

(20) Bouvry, B.; Fernandez Carrion, A. J.; Andujar, J.; Veron, E.; Ory, S.; Brassamin, S.; Echegut, P.; Escape, C.; Nahhas, T.; Py, X.;

Bessada, C. Mediterranean basin basalts as potential materials for thermal energy storage in concentrated solar plants. *Sol. Energy Mater. Sol. Cells* **2017**, *171*, 50−59.
(21) Aladejare, A.; Wang, Y. Evaluation of rock property variability. *Georisk* **2017**, *11*, 22.
(22) Begg, G.C.; Griffin, W.L.; Natapov, L.M.; O'Reilly, S. Y.; Grand, S.P.; O'Neill, C.J.; Hronsky, J.M.A.; Djomani, Y. P.; Swain, C.J.; Deen, T.; Bowden, P.; et al. The lithospheric architecture of Africa: Seismic tomography, mantle petrology, and tectonic evolution. *Geosphere* **2009**, *5*, 23−50.
(23) James, D.; Fouch, M. Formation and evolution of Archaean cratons: Insights from southern Africa. *Geological Society, London, Special Publications* **2002**, *199*, 1−26.
(24) Kabete, J.; McNaughton, N.; Groves, D.; Mruma, A. H. Reconnaissance SHRIMP U−Pb zircon geochronology of the Tanzania Craton: evidence for Neoarchean granitoid−greenstone belts in the Central Tanzania Region and the Southern East African Orogen. *Precambrian Research* **2012**, *216*, 232−266.
(25) Sun, K.; Zhang, L.-l.; Zhao, Z.-d.; He, F.-q.; He, S.-f.; Wu, X.-y.; Qiu, L.; Ren, X.-d. Episodic crustal growth in the Tanzania Craton: evidence from Nd isotope compositions. *China Geology* **2018**, *1* (2), 210−224.
(26) GST. *Explanatory notes for the minerogenic map of Tanzania*; Geological Survey of Tanzania, 2015.
(27) Fritz, H.; Tenczer, V.; Hauzenberger, C.; Wallbrecher, E.; Hoinkes, G.; Muhongo, S.; Mogessie, A. Central Tanzanian tectonic map: a step forward to decipher Proterozoic structural events in the East African Orogen. *Tectonics* **2005**, *24* (6), No. 1796, DOI: 10.1029/2005TC001796.
(28) Sommer, H.; Kröner, A. Ultra-high temperature granulite-facies metamorphic rocks from the Mozambique belt of SW Tanzania. *Lithos* **2013**, *170*, 117−143.
(29) Moeller, A.; Appel, P.; Mezger, K.; Schenk, V. Evidence for a 2 Ga subduction zone: Eclogites in the Usagaran belt of Tanzania. *Geology* **1995**, *23*, 1067.
(30) Chen, C.; Zhu, C.; Zhang, B.; Tang, B.; Li, K.; Li, W.; Fu, X. Effect of Temperature on the Thermal Conductivity of Rocks and Its Implication for In Situ Correction. *Geofluids* **2021**, *2021*, No. 6630236.
(31) Hongois, S.; Kuznik, F.; Stevens, P.; Roux, J.-J. Development and characterisation of a new MgSO4−zeolite composite for long-term thermal energy storage. *Sol. Energy Mater. Sol. Cells* **2011**, *95* (7), 1831−1837.
(32) Srivastava, P.; Krishna, A.; Jawed, S.; Sarkhel, P. Quantitative minerological analysis of some granite rocks of deoghar jharkhand. *Earth Sci. Res.* **2020**, *9*, 30.
(33) Abdollahnejad, Z.; Mastali, M.; Rahim, F.; Luukkonen, T.; Kinnunen, P.; Illikainen, M. Influence of cobinders on durability and mechanical properties of alkali-activated magnesium aluminosilicate binders from soapstone. In *New Materials in Civil Engineering*; Samui, P., Kim, D., Iyer, N. R., Chaudhary, S., Eds.; Butterworth-Heinemann, 2020; Chapter 29, pp 877−895.
(34) Hartlieb, P.; Toifl, M.; Kuchar, F.; Meisels, R.; Antretter, T. Thermo-physical properties of selected hard rocks and their relation to microwave-assisted comminution. *Minerals Engineering* **2016**, *91*, 34−41.
(35) ASTM. *Annual Book of ASTM Standards*; American Society for Testing and Materials, 2013.
(36) Rybacki, E.; Reinicke, A.; Meier, T.; Makasi, M.; Dresen, G. What controls the mechanical properties of shale rocks? − Part I: Strength and Young's modulus. *J. Pet. Sci. Eng.* **2015**, *135*, 702−722.
(37) Borodich, F. M.; Bull, S. J.; Epshtein, S. A. Nanoindentation in studying mechanical properties of heterogeneous materials. *Journal of Mining Science* **2015**, *51* (3), 470−476. Ma, Z.; Pathegama Gamage, R.; Zhang, C. Application of nanoindentation technology in rocks: a review. *Geomechanics and Geophysics for Geo-Energy and Geo-Resources* **2020**, *6* (4), 60.
(38) Oliver, W. C.; Pharr, G. M. An improved technique for determining hardness and elastic modulus using load and displacement sensing indentation experiments. *J. Mater. Res.* **1992**, *7* (6), 1564−1583. From Cambridge University Press Cambridge Core.
(39) Strecker, K.; Panzera, T.; Sabariz, A.; Miranda, J. The effect of incorporation of steatite wastes on the mechanical properties of cementitious composites. *Materials and structures* **2010**, *43* (7), 923−932.
(40) Baron, A.; Burke, A. L.; Gratuze, B.; Chapdelaine, C. Characterization and origin of steatite beads made by Northern Iroquoians in the St. Lawrence Valley during the 15th and 16th centuries. *Journal of Archaeological Science: Reports* **2016**, *8*, 323−334.
(41) Maqsood, A.; Kamran, K.; Gul, I. H. Prediction of thermal conductivity of granite rocks from porosity and density data at normal temperature and pressure: in situ thermal conductivity measurements. *J. Phys. D: Appl. Phys.* **2004**, *37* (24), 3396.
(42) Srinivasan, S.; Dodson, D.; Charles, M. B. J.; Wallen, S. L.; Albarelli, G.; Kaushik, A.; Hickman, N.; Chaudhary, G. R.; Stefanakos, E.; Dhau, J. Energy Storage in Earth-Abundant Dolomite Minerals. *Applied Sciences* **2020**, *10* (19), 6679. Yavuz, H.; Demirdag, S.; Caran, S. Thermal effect on the physical properties of carbonate rocks. *International Journal of Rock Mechanics and Mining Sciences* **2010**, *47* (1), 94−103.
(43) Manya, S.; Maboko, M. A. H. Generation of Palaeoproterozoic tonalites and associated high-K granites in southwestern Tanzania by partial melting of underplated mafic crust in an intracontinental setting: Constraints from geochemical and isotopic data. *Lithos* **2016**, *260*, 120−133.
(44) Jones, M. Thermal properties of stratified rocks from Witwatersrand gold mining areas. *Journal of the Southern African Institute of Mining and Metallurgy* **2003**, *103* (3), 173−185.
(45) Gabert, G. Lithostratigraphic and tectonic setting of gold mineralization in the Archean cratons of Tanzania and Uganda, East Africa. *Precambrian research* **1990**, *46* (1−2), 59−69.
(46) Jones, M. Thermal properties of stratified rocks from Witwatersrand gold mining areas. *Journal of the Southern African Institute of Mining and Metallurgy* **2003**, *103* (3), 185 DOI: 10.1002/srin.202000687.
(47) Hrifech, S.; Agalit, H.; Bennouna, E. G.; Jarni, A.; Mouguina, E. M.; Mimet, A. Preliminary characterizations of natural rocks as storage materials for a medium range temperature TES. *AIP Conf. Proc.* **2019**, *2123* (1), No. 020091. (acccessed 2022/08/07).
(48) Huhta, A. Diversity of soapstones: Classification and thermal behavior. Ph.D. Dissertation, University of Oulu, 2019.
(49) Hänchen, M.; Brückner, S.; Steinfeld, A. High-temperature thermal storage using a packed bed of rocks − Heat transfer analysis and experimental validation. *Applied Thermal Engineering* **2011**, *31* (10), 1798−1806.
(50) Zhu, Z.; Tian, H.; Jiang, G.; Dou, B. Effects of high temperature on rock bulk density. *Geomechanics and Geoengineering* **2022**, *17* (2), 647−657.
(51) Vosteen, H.-D.; Schellschmidt, R. Influence of temperature on thermal conductivity, thermal capacity and thermal diffusivity for different types of rock. *Physics and Chemistry of the Earth, Parts A/B/C* **2003**, *28* (9), 499−509.

https://doi.org/10.1021/acsomega.3c00314
ACS Omega 2023, 8, 18554−18565